Published in final edited form as:
Chem Soc Rev. 2012 January 21; 41(2): 608–621. doi:10.1039/c1cs15112f.

Misfolded Proteins in Alzheimer's Disease and Type II Diabetes

Alaina S. DeToma[a,§], **Samer Salamekh**[a,§], **Ayyalusamy Ramamoorthy**[a,b,*], and **Mi Hee Lim**[a,c,*]

[a]Department of Chemistry, University of Michigan, Ann Arbor, Michigan, 48109 (USA)

[b]Department of Biophysics, University of Michigan, Ann Arbor, Michigan, 48109 (USA)

[c]Life Sciences Institute, University of Michigan, Ann Arbor, Michigan, 48109 (USA)

Abstract

This review presents descriptions of two amyloidogenic proteins, amyloid-β (Aβ) peptides and islet amyloid polypeptide (IAPP), whose misfolding propensities are implicated in Alzheimer's disease (AD) and type II diabetes, respectively. Protein misfolding diseases share similarities, as well as some unique protein-specific traits, that could contribute to the initiation and/or development of their associated conditions. Aβ and IAPP are representative amyloidoses and used to highlight some of the primary considerations for studying misfolded proteins associated with human diseases. Among these factors, their physiological formation, aggregation, interactions with metal ions and other protein partners, and toxicity are presented. Small molecules that target and modulate the metal-Aβ interaction and neurotoxicity are included to illustrate one of the current approaches for studying the complex nature of misfolded proteins at the molecular level.

Introduction

The accumulation of misfolded proteins is a hallmark feature in numerous human disorders including blood diseases like sickle cell anemia, neurodegenerative diseases such as Alzheimer's diseases (AD) and Parkinson's disease (PD), and metabolic diseases such as type II diabetes.[1-4] Misfolded protein aggregates may deposit intracellularly or extracellularly in tissues. The conformational changes accompanying misfolding can result in disruption of the regular function of the protein or may result in a gain of function that is often associated with toxicity. Amyloid peptides represent a subset of misfolded proteins that share unique characteristics.[5,6] Attributes common to amyloids include the appearance of linear growth of water-insoluble aggregates when viewed under an electron microscope (EM), a unique X-ray diffraction pattern, and affinity for amyloid-sensitive dyes (congo red and thioflavin-T (ThT)).[5,6] Mature fibrils observed by EM are composed of protofibrils having a β-sheet conformation, with the direction of the β-strands perpendicular to the fibril axis that laterally associate with monomers or other protofibrils.[6–9]

The aggregation of amyloids is a cooperative process that in general adheres to a "nucleation-dependent polymerization" model involving two phases: a lag phase and an elongation phase (Fig. 1).[6–8] According to the model, the peptide transiently self-associates into small oligomeric species during the lag time.[8] Near the end of the lag phase, a thermodynamically unfavorable nucleus forms and is used as a template for fibril growth in the elongation period.[8] A trace of this aggregation process is generally sigmoidal (Fig. 1). The two-phase kinetics can be tracked by observing the increased fluorescence of amyloid

*To whom correspondence should be addressed: ramamoor@umich.edu and mhlim@umich.edu.
§These authors contributed equally to this work.

sensitive dyes, increased β-sheet secondary structure measured by circular dichroism spectroscopy (CD) and Fourier transform infrared spectroscopy (FTIR), decreased molecular tumbling measured by intrinsic fluorescence anisotropy (for amyloids containing fluorescent residues), or time-lapsed observation of the peptide morphology by atomic force microscopy (AFM).[10]

Characterization of monomeric and fibrillar species has provided significant insights into the conformational changes accompanying the aggregation process of an amyloid protein; however, the transient nature of oligomers and the heterogeneity of conformations existing in equilibrium with oligomers have challenged traditional characterization methods. Soluble amyloid peptides can be stabilized by lowering the temperature, incubating with detergents or lipids, adding a small amount of denaturant, altering the local pH away from the isoelectric point (where the peptide is least soluble), using mutants, and/or using small molecule inhibitors.[6] The fibrillar form of the peptide is thermodynamically more favorable than the monomeric or oligomeric forms and can readily be stabilized if allowed to equilibrate.[6,11] On the other hand, far fewer methods exist for stabilizing oligomers, with chemical cross-linking being one of the most common methods.[12] Instead, indirect approaches to studying oligomers are employed. These include molecular dynamics (MD) simulations and analysis of aggregation traces. For example, the observation that a trace amount of helix-promoting solvent decreases the lag times of amyloids discussed in this review has led to the hypothesis that the aggregation pathway involves helical intermediates.[13,14] By using high concentrations of a helix promoting solvent (> 20%), the protein can be stabilized in a helical conformation to indirectly study these proposed intermediates. Elucidation of the aggregation pathways is further complicated by the presence of off-pathway species that do not lead to the fibril formation, particularly in the presence of small molecule inhibitors.[15,16] Consequently, oligomerization and fibrillization possibly can occur *via* distinct mechanisms that could have profoundly different outcomes *in vivo*.[15,16]

Significant research efforts to comprehensively and coherently summarize how and why misfolded proteins are so intimately associated with human diseases have been pursued, especially as it pertains to two severe health crises, AD and type II diabetes. According to the Centers for Disease Control and Prevention, AD and diabetes were the sixth and seventh leading causes of death in the United States in 2007, respectively, attesting to the tremendous efforts to understand the etiology of these diseases in recent years.[17] Although the primary defects in diabetes and AD are localized in different tissues, epidemiological studies have shown that the two diseases share risk factors (*e.g.*, obesity, high cholesterol, high blood pressure), and diabetics have an increased risk for developing AD.[18,19]

While it is accepted that the amyloid proteins, amyloid-β (Aβ) and the islet amyloid polypeptide (IAPP), are key players in AD and type II diabetes, respectively, several questions surrounding these amyloidogenic proteins remain unclear: (a) which conformation is directly responsible for pathogenesis of the amyloid peptides?; (b) what are critical elements for aggregation in biological systems that facilitate amyloid toxicity and are they drug targets?; (c) what are critical elements for aggregation in biological systems that ameliorate amyloid toxicity and what is their role in etiology of associated diseases? The intention of this review is to employ Aβ and IAPP as models for exploring the factors associated with protein misfolding that could play vital roles in aging amyloid diseases.

1. Alzheimer's Disease (AD) and Amyloid-β (Aβ)

AD is the most prevalent form of neurodegeneration that is associated with severe cognitive impairment and memory loss primarily among elderly adults. Currently, over 5 million

Americans are afflicted by AD, placing a severe burden on socioeconomic resources.[20] Although the symptomatic and pathological signs of AD have been identified, a complete understanding of their origins remains elusive. This uncertainty has impeded progress toward developing effective preventive and disease modifying therapeutics; the presently available drugs alleviate the symptomatic burdens temporarily and are unable to deter or cure the disease.[20–22] While some cases of AD are attributed to genetic inheritance, the majority of cases are sporadic.[21] Confirmation of the AD diagnosis is contingent upon the identification of misfolded protein aggregates, including the neurofibrillary tangles composed of hyperphosphorylated tau protein and senile plaques composed of Aβ peptides, as well as extensive oxidative damage and neuronal loss in the brain *post mortem*.[21,22] Within the mature plaques from diseased brains, high concentrations of metals such as Fe, Cu, and Zn are also found. Along with studies identifying dyshomeostasis and miscompartmentalization of these metal ions in the diseased brain, this finding implies that along with protein aggregate accumulation, metals may contribute to AD onset and progression.[22–30] Taken together, misfolded Aβ species, metal ion dyshomeostasis/miscompartmentalization, and oxidative stress partially represent AD etiology.[21–30] In the present section, we survey the generation and aggregation of Aβ and the role of metal ions in AD and Aβ-related events. A discussion of the development of multifunctional small molecules is also provided to illustrate current approaches to understand the nature of the metal-Aβ interaction and its potential contributions to AD.

1.1 Amyloid Precursor Protein (APP) and Aβ Generation

The Aβ peptide is the predominant component of the senile plaques that accumulate in various brain regions and pathologically represent the AD condition.[1–3,21–25,27–29,31] Its involvement in AD neuropathogenesis has been extensively studied following the establishment of the amyloid cascade hypothesis, which implicates Aβ as a causative agent in AD.[31] The Aβ peptide is composed of 38–43 amino acid residues and is generated through sequential proteolytic cleavage of the amyloid precursor protein (APP) (Fig. 2).[21,22,32] APP is a transmembrane protein with three common isoforms, APP_{695}, APP_{751}, and APP_{770}, which among them, APP_{695} is most common in the neuronal cells.[21,32] The function of APP is still incompletely defined, but with metal binding domains localized near APP residues 124–189 and residues from 672–713 (approximate Aβ region from APP_{770} isoform), it has been suggested that APP could be involved in regulating metal ion (*e.g.*, Cu) transport and homeostasis.[30,32,33] A recent report has demonstrated that APP exhibits ferroxidase activity in a similar manner to that of ceruloplasmin (a Cu transport protein) whereby APP facilitates Fe export from neuronal cells; inhibition of this activity by reserves of Zn(II) could be connected to elevated levels of Fe measured in AD (*vide infra*).[34]

The proteases responsible for APP cleavage and Aβ generation distinguish the resulting forms of Aβ as either non-amyloidogenic or amyloidogenic (disease-related) (Fig. 2).[21,22,30,32] Processing of APP by α-secretase initiates the non-amyloidogenic cleavage pathway, with initial scission between K687 and L688 (APP_{770} numbering) affording a large soluble fragment (sAPPα) and leaving a portion of the parent APP molecule membrane-bound (Fig. 2). On the other hand, the amyloidogenic pathway begins with APP cleavage by β-secretase (β-site APP cleaving enzyme, BACE1) nearer to the *N*-terminus of APP between residues M671 and D672. The remaining membrane-bound fragments from both paths are finally processed by γ-secretase, which requires four protein components for its activity: presenilin (PS1 or PS2), nicastrin, anterior pharynx-defective-1 (APH-1), and presenilin enhancer-2 (PEN-2).[21,32,35] The γ-secretase complex cleaves the *C*-terminal fragments within the membrane to produce monomeric Aβ peptides of varying lengths and amyloidogenic preferences. The common full-length peptides, $Aβ_{1-40}$ and $Aβ_{1-42}$, are produced through the amyloidogenic pathway (the amino acid sequence of $Aβ_{1-42}$ is

DAEFRHDSGYEVHHQKLVFFAEDVGSNKGAIIGLMVGGVVIA) (Fig. 2). Monomeric Aβ tends to aggregate, forming low molecular weight (LMW) Aβ species, oligomers, protofibrils, and fibrils as previously described (*vide supra*; Fig. 1).

1.2 Aggregated Aβ Species and Their Contribution to Neurotoxicity

Aβ is a relatively small peptide for which the innate function has not been fully established. The structure of Aβ monomer features hydrophilic *N*-terminus and hydrophobic *C*-terminus, which play a role in driving its aggregation in an effort to minimize unfavorable interactions with the aqueous environment.[22] Residues contained in the region from L17–A21 are identified as key contributors to self-recognition, due to their primarily hydrophobic nature, which might be influential in producing the higher-order structures.[22,36] Fibrils of $A\beta_{1\text{-}40}$ adopt β-strand characteristics in two regions, from residues 12–24 and 30–40 and their side chain interactions stabilize the cross-β sheet within the fibrillar structure.[37] Within the peptide, a turn occurs in the region from G25–G29 that is stabilized by a combination of electrostatic interactions such as a salt bridge between D23 and K28.[22,36,37]

$A\beta_{1\text{-}42}$ is the primary constituent of the senile plaques; the two additional hydrophobic residues at the *C*-terminus enhance its tendency to aggregate over $A\beta_{1\text{-}40}$, although the shorter peptide ($A\beta_{1\text{-}40}$) accounts for the major product of γ-secretase cleavage yielding Aβ peptides.[21,22] Aβ undergoes conformational changes during aggregation where the native random coil structure can be modified to either α-helical or β-strand-like forms.[36] The conformational changes, however, are highly conditional and slight changes in parameters such as pH, peptide concentration, environmental composition, and metal ion concentration may lead to diverse amyloid aggregates that may be ordered or may be amorphous.[9,23] The array of known polymorphic forms of Aβ aggregates aside from the monomers and fibrils, which includes oligomers, protofibrils, annular structures, Aβ-derived diffusible ligands (ADDLs), and globulomers, has recently been reviewed.[9]

It is still not clear which Aβ conformation is directly linked to neuropathogenesis. Some recent evidence implicates soluble LMW Aβ species, such as dimers, instead of the plaques as the relevant neurotoxic species.[3,22,35,38] In the early stages of AD, reduced synaptic function and impairment of learning and memory formation processes (*e.g.*, long-term potentiation) may be caused by the smaller Aβ assemblies, such as oligomers or ADDLs; these species possibly interfere with neurotransmission and/or other signaling pathways in the cells.[35] The occurrence of physiological responses in the brain such as inflammation and neuronal death as the disease progresses, however, could be attributable to these soluble aggregated species, the plaques, or a combination of various species in association with each other. Additional mechanisms proposed for the toxicity of Aβ aggregates are related to interactions with other biomacromolecules (*e.g.*, pore formation within lipid membranes) and oxidative stress (*e.g.*, lipid peroxidation).[22,35]

1.3 Metal Ions in AD and their Interactions with Aβ

Metal ions have important physiological contributions throughout the body, including structural, catalytic, and signaling functions, and they are typically well regulated to prevent detrimental effects.[23] Essential transition metal ions, such as Cu(I/II) and Zn(II), have important functions in the brain, such as communication of information between neurons at the synapse. For example, Zn(II) is co-released with glutamate during neuronal stimulation and taken up by Ca(II) channels where it can then participate in intracellular signaling events.[39] Maintaining the appropriate balance of metal ions (homeostasis) in the brain is critical for healthy brain function and is well regulated by the blood-brain barrier (BBB).[39] With increasing age and/or oxidative stress, however, the BBB can become compromised such that both necessary (*e.g.*, Fe, Cu, and Zn) and unnecessary metals (*e.g.*, Al) are more

easily transported into or out of the brain.[23,25,39] As a result, localization may be disrupted, and consequently, homeostasis of the former set may be affected. Among the metals found in the body, those that are of most concern in AD include the transition metals Fe, Cu, and Zn. Due to the association of high levels of these metals with Aβ aggregates from diseased brain tissues, Fe, Cu, and Zn have been suspected to be linked to the pathological events of AD.[21–24,40–43]

In particular, Cu(I/II) and Zn(II) have recently garnered attention for being able to directly bind to the Aβ peptides.[21–24,40–43] Both metals are usually found in association with biological ligands, but a pool of "free" (*i.e.*, chelatable) ions can exist in the synaptic cleft.[25,27,40] The concentrations of Cu(II) and Zn(II) can reach up to 15 μM and 300 μM, respectively, in the glutamergic synapses during neurotransmission, from which only a fraction may be sufficient to be related to the disease pathology.[23,25,39,40] The estimated levels of metals in the Aβ plaques are in the high micromolar to low millimolar range, with total plaque content being reported at *ca.* 0.9 mM for Fe, 0.4 mM for Cu, and 1 mM for Zn.[23,25,26,41] Although Fe is abundant in the plaques, it does not co-purify with peptides from the AD brain tissue in the same manner as Cu and Zn hinting that its role in AD may not be related to direct coordination to the peptide.[23] Instead, in the case of Fe, as well as Cu, the other potential factor for AD pathology is their involvement in promoting an imbalance of reactive oxygen species (ROS) generated through Fenton chemistry, which leads to oxidative stress (Fig. 3).[22–24,26,28,29]

Despite the uncertain nature of the metal-Aβ interaction *in vivo*, it has been established that metal ions are able to bind to Aβ *in vitro* (Fig. 1).[22,23,30,42–44] Both Cu(II) and Zn(II) have been shown to bind to Aβ in a 1:1 fashion, although it has been also reported that Aβ can bind up to approximately two equivalents of Cu(II). The coordination environment of the Cu(II) and Zn(II) has been investigated using an array of spectroscopic methods including nuclear magnetic resonance spectroscopy (NMR), electron paramagnetic resonance spectroscopy (EPR), UV-visible spectroscopy, CD, and X-ray absorption spectroscopy (XAS).[30,40,42–45] Several probable coordination modes have been proposed, but the exact identity of the ligands for these ions has not been fully elucidated. The current evidence suggests a binding environment containing a mixture of nitrogen and oxygen donor atoms for both Cu(II) and Zn(II), for which three histidine residues (H6, H13, and H14) are likely to be included.

The previous studies of Cu-bound Aβ monomers suggest several metal binding features, which have been not fully characterized given the complexity of the solution speciation measured under various experimental conditions.[23,30,40,42–44] First, two separate metal binding sites in the peptide may be possible. Second, depending on the oxidation state of Cu (*e.g.*, Cu(I) or Cu(II)), different binding modes and coordination environments on the metal center have been observed. To date, however, relatively little has been uncovered to identify the coordination mode for Cu(I) over Cu(II). This area has attained more interest recently as the reducing conditions found in the brain make the redox cycling of Cu, and therefore the coordination environment of Cu(I), a physiologically relevant concern.[42,44,46,47] Finally, the coordination environment of Cu(II)-bound Aβ is dynamic and likely contingent upon pH, which has precluded an absolute assignment of the binding ligands and/or geometry.[30,42–44] In the physiologically relevant range (*ca.* pH 7.4), Aβ tends to involve three nitrogen and one oxygen (3N1O) donor atoms coordinated to Cu, commonly referred to as "component I". The donor atoms are possibly derived from three histidine residues (H6, H13, and H14) along with the carboxylate of D1 or from two histidine residues and both the amine and carboxylate of the *N*-terminus.[30,42–44,48] When the pH is raised above *ca.* pH 8, there is evidence of a different coordination sphere, deemed "component II." At this condition, metal binding seems to occur in a similar manner (*i.e.*, 3N1O) as "component I" but uses the

main chain carbonyl of A2 in conjunction with the three histidine residues for metal binding or a mixture of an *N*-terminal amine, deprotonated backbone amide N, carbonyl, and a histidine residue as ligands.[43,44,49] Alternatively, a 4N coordination mode has been proposed for "component II" that may involve an *N*-terminal amine or a deprotonated backbone amide as a N donor source in addition to H6, H13, and H14.[30,43,44] The present understanding of how Cu(II) directly interacts with Aβ has been detailed in a recent review by Drew and Barnham.[44] While Cu(II)-Aβ complexes likely form a four-coordinate species, Zn(II)-Aβ may coordinate four to six ligands. There is a consensus that the three histidine residues are responsible for binding; however, the fourth, fifth, and/or sixth ligands have been more difficult to identify.

Metal binding to Aβ has been suggested to initiate peptide aggregation and neurotoxicity.[21–30,40,42,43] When considering the Aβ aggregation according to the nucleation polymerization model (*vide supra*, Fig. 1), the formation of the initial nucleus and subsequent elongation into the familiar cross-β-sheet nature of the fibrils tends to be a rather slow process in quiescent, metal-free conditions *in vitro*; however, in the presence of metal ions like Cu(II) and Zn(II), the aggregation kinetics can be accelerated.[40,50] Substoichiometric amounts of Cu(II) have been shown to reduce fibril generation time by half pH 7.4 as a result of the peptide nearing its isoelectric point.[50] Cu(II) also facilitates Aβ aggregation under slightly acidic conditions. Treatment of Aβ with micromolar concentrations of Zn(II) leads to insoluble amorphous peptide species in a rapid process occurring within milliseconds.[51] In both cases, aggregation is initiated by monomeric metal-Aβ complexes.

Through calorimetric and spectroscopic methods, dissociation constants (K_d) indicative of the binding affinity of metal ions to Aβ have been reported.[23,40,42,43] For Cu(II), the reported K_d values range from attomolar to nanomolar. On the other hand, the affinity of Aβ for Zn(II) is weaker; it is found on the order of micromolar concentrations. The length of Aβ does not significantly impact these binding affinities in $Aβ_{1-40}$ *versus* $Aβ_{1-42}$, and similar affinities are measured for the monomer and pre-formed Aβ aggregates; however, the experimental conditions used to attain these data can dramatically influence the outcomes.[43] Nevertheless, it is valuable to be aware of the approximate range of the dissociation constants for metal ions with Aβ. Such information may be helpful for selecting chemical tools that are directed toward the metal ions associated with various Aβ species. In general if the small molecules have similar affinity for metal ions as Aβ (approximately within the same order of magnitude), then there exists a possibility for competition between the ligand and peptide for metal binding/chelation (*vide infra*).[43,52–54]

Another effect of metal binding to Aβ in AD includes the exacerbation of neurotoxicity.[21–30,40,42,43] Toxicity has been demonstrated to be higher for Cu-Aβ species *in vitro*, particularly because the Fenton-type redox cycling between Cu(II) and Cu(I) is sustainable under the reducing environments of the brain (Fig. 3). ROS produced from this chemistry, such as hydrogen peroxide (H_2O_2) and hydroxyl radical, can cause oxidative damage to biological molecules and membranes (*e.g.*, lipid peroxidation). Furthermore, ROS accrual may overwhelm the endogenous antioxidant defense systems in the cell that could ultimately lead to cell death.

1.4 Small Molecule-Based Approaches to Understanding Metal-Aβ Interaction and Neurotoxicity

Even though concentrated areas of metal ions (Cu/Zn) have been observed in AD brains and many studies have indicated deleterious effects caused by metal binding, the relationship between Cu/Zn-Aβ interaction and AD remains to be clarified. The pursuit of small molecules as chemical tools to interrogate the metal-Aβ interaction and associated events

such as aggregation and neurotoxicity may provide a handle for further dissecting the etiology of this disease. Not only could effective compounds lead to new molecular-level insights but they may also be promising chemical candidates for developing potential AD therapeutics. For this purpose, metal chelation therapy has been explored by employing general metal chelating compounds to remove or potentially block these metal ions from interacting with Aβ to alleviate aggregate deposition and ROS production (Fig. 4; *e.g.*, CQ, EDTA).[21–25,55,56] From this approach, the potential roles of metal ions in AD have been acknowledged and new methods to design compounds for potentially elucidating how metal-associated Aβ species (metal-Aβ species) are connected to the neuropathology of AD have been explored.

Investigations with 8-hydroxyquinoline derivatives, CQ (Fig. 4) and PBT2, *in vitro* and *in vivo* have suggested their ability to interrupt the associations between metal ions and Aβ, to sequester redox active metal ions, and to transport metal ions across the membrane leading to their redistribution (*i.e.,* ionophore activity).[23–25,55] Due to limited utility and adverse effects of CQ,[23,25,55] its analogue PBT2 has been of recent interest as it leads to better ionophore behavior, greater depletion of amyloid deposits, and improved performance on neuropsychological tests in AD patients. These observations have provided evidence that metal homeostasis is severely misregulated in AD and that mitigating this dyshomeostasis may be of therapeutic value. Although showing progress and lending credibility to metal ion chelation therapy in AD, these 8- hydroxquinoline compounds have disadvantages for probing the direct correlation between Aβ and metal ions due to the lack of Aβ recognition functionality, which may result in alteration of biological metal ion homeostasis rather than metal ions within Aβ species.[24,25,52,55,57] Therefore, rational structure-based design approaches have been attempted for the construction of more versatile metal chelators containing additional modes of action for specifically targeting and elucidating the role of metal ions associated with Aβ.

Expanding upon the concept of metal chelation, multifunctional compounds that incorporate various functionalities for direct Aβ interaction, ROS mediation, or improved BBB permeability in tandem with capturing metals ions have evolved. Combining more than one function into a single molecule may assist in localizing compounds near metal-Aβ species in the brain (Fig. 4).[23,52,57,58] For one of these classes, the strategy has been to promote metal complexation by increasing the number of donor atoms to generate multidentate ligand frameworks.[59] Along with sequestration of the redox active metal ions (*e.g.*, Cu(I/II)) from Aβ species, multidentate ligands can produce the geometry of the metal center that disfavors the transition between oxidation states.[59] Another approach is to prepare prochelators with concealed metal binding sites that in principle prevent unwanted systemic metal coordination and only become active metal scavengers upon reaching a biological target or stimulus (*e.g.*, enzymes, ROS).[23,58,60–62] In one prochelator framework, a boronic acid masks the hydroxyl group of 8- hydroxyquinoline (QBP; Fig. 4) until activation by H_2O_2 resulting in the cleavage of the boron protecting group. In the presence of redox active Cu-Aβ and O_2, the production of H_2O_2 will stimulate the delivery of 8-hydroxyquinoline, which can chelate metal ions, mitigate ROS production, and reduce metal-induced Aβ aggregation *in vitro*.[60] Orvig and coworkers have developed a family of glycosylated 3-hydroxy-4-pyridinones capable of metal binding and antioxidant activity upon cleavage of the sugar group (Fig. 4).[61] Inclusion of the sugar moiety would exploit GLUT-1 transporters at the BBB allowing for more facile penetration into the brain whereby it could be readily hydrolyzed by β-glucosidase enzymes to reveal the active chelators. These compounds have demonstrated comparable antioxidant activity to α-tocopherol (vitamin E) and were able to solubilize metal-induced Aβ aggregates. Taking this approach one step further, pyridinone glycoside derivatives that also include Aβ interaction moieties have been recently reported (Fig. 4).[62] Combining prochelation, BBB permeability, antioxidant activity, and Aβ

recognition functionalities successfully within one molecule is attractive for not only understanding the relationship of metal-Aβ and neurotoxicity in AD but is also promising as a future therapeutic direction.

The third and possibly more direct combination for designing multifunctional compounds that can specifically target metal ions associated with Aβ species is the installation of metal chelation properties into molecules previously determined to interact with Aβ. This strategy has branched into two similar approaches through synthetic manipulation: linkage and incorporation.[23,52,57,58] In the first case, either a small molecule Aβ imaging agent or a complementary peptide recognition sequence (*e.g.*, KLVFF) is tethered to a metal chelating framework (*e.g.*, ThT-based compound XH1, Fig. 4).[63,64] In the second approach, a metal chelation site is directly placed into the known Aβ recognition framework. Molecules from the second strategy include modified neutral ThT derivatives (*e.g.*, HBT; Fig. 4) and two generations of compounds based on the stilbene and IMPY frameworks that present different degrees of biocompatibility and reactivity toward metal-Aβ species (*e.g.*, L2-b, K1; Fig. 4).[23,52–54,57,58,65,66] Another recent discovery by Lim and coworkers was that a naturally occurring compound from the flavonoid family, myricetin, can be classified as a bifunctional molecule with utility in targeting and modulating metal-Aβ aggregation and neurotoxicity *in vitro*.[67] Overall, the multifunctionality of these compounds has been demonstrated *in vitro* and in living cells based on their ability to block metal-induced Aβ aggregation, to reverse the degree of amyloid aggregation, to attenuate ROS production, and to prevent toxicity from metal-Aβ species. Limited *in vivo* studies have been conducted with the designed compounds so far (*i.e.*, XH1 reduced amyloid burden in a double-transgenic mouse model), and one study showed the ability of L2-b to disassemble biologically derived high molecular weight Aβ species from human AD brain tissue homogenates.[54,57,63] Toward applications to understand the role of metal ions associated with Aβ in AD, these strategies motivated by metal chelation are in promising initial stages. The attempts thus far to rationally design multifunctional molecules have provided a foundation on which the details of metal-Aβ interaction may be revealed more completely and applied to the comprehensive picture of the nature of AD.

2. Type II Diabetes and Islet Amyloid Polypeptide (IAPP)

Diabetes mellitus is a degenerative metabolic disease characterized by progressive loss of glucose homeostasis, affecting more than 170 million people worldwide.[68] Diabetes encompasses a range of metabolic disorders; however, the most common classifications are type I, or “juvenile” diabetes and type II, or “adult-onset,” diabetes. The primary defect in type I diabetics is a loss of insulin-producing pancreatic β cells often caused by a T-cell mediated autoimmune attack on β cells. Initial stages of type II diabetes are characterized by elevated levels of circulating insulin as insulin-secreting β cells attempt to overcome systemic insulin resistance.[69,70] Left untreated, later stages of the disease are characterized by failure of insulin-producing pancreatic β cells and complications associated with hyperglycemia. Type II diabetes is the most common form of diabetes, affecting approximately 90% of diabetics in the United States, and is the focus of this section of the review.[69]

The underlying biochemical defects of type II diabetes have not been fully elucidated; however, early studies of β cells from type II diabetics revealed the presence of proteinaceous plaques in 90% of patients that were absent in healthy individuals.[70] These plaques are primarily composed of a protein called the islet amyloid polypeptide (IAPP) and the peptide is secreted in both healthy individuals and diabetics. The causal link between IAPP and type II diabetes was strengthened following the discovery that overweight

transgenic mice readily developed symptoms characteristic of type II diabetes after over-expressing the human IAPP variant.[71]

Human IAPP (hIAPP) is a 37-residue amyloidogenic peptide hormone secreted primarily by pancreatic β-cells in the islets of Langerhans in response to high glucose levels.[70] The peptide is secreted with insulin simultaneously and has been shown to enhance the effects of insulin by slowing gastric emptying, reducing the rate of glucose entering the blood, and signaling the brain to reduce meal size.[72] The peptide, however, has a concentration-dependent amyloidogenic propensity that causes membrane disruption, channel formation, and cellular toxicity.[8] The resulting insoluble plaques have the characteristic β-sheet structure of amyloidogenic proteins and respond similarly to congo red as other amyloid proteins (*vide supra*).[70]

Unlike Aβ, where differing cleavage sites result in peptides with varying amyloidogenic propensities, the same hIAPP sequence is synthesized and secreted in healthy individuals and type II diabetics.[71] Therefore, there must exist mechanisms in healthy individuals that regulate its tendency to aggregate and protect against the observed cytotoxicity. The low picomolar concentration of hIAPP in the blood does not appear to be sufficient to induce self-aggregation; however, the peptide is found in low millimolar concentrations in intracellular secretory granules of pancreatic β cells.[73] *In vitro*, millimolar concentrations of hIAPP aggregate within minutes, but the turnover of β cells granules is slower *in vivo* (on the order of hours).[74] Therefore, it is reasonable to look for factors in the secretory granule that prevent the aggregation and aggregation related toxicity of hIAPP. The second part of this review describes an overview of three factors found in the secretory granule that have been shown to affect hIAPP toxicity in model systems: pH, metal ion levels, and interactions with other proteins.

2.1 Effect of pH on IAPP Aggregation

The acidic pH (*ca.* 5) of the secretory granule of β cells has been shown to inhibit hIAPP fibrillization *in vitro*.[74] Previous studies revealed a general trend where amyloid fibril formation is maximized at pH values where the solubility of the peptide was at a minimum (*i.e.*, the isoelectric point).[75] The slow aggregation of hIAPP in the acidic conditions of the secretory granule is therefore likely due to the shift in solubility as the pH deviates from the isoelectric point of 8.9 for hIAPP.[76]

Direct determination of the effect of pH on hIAPP-mediated cellular toxicity provides a challenge as β cell viability decreases substantially with deviation from physiological pH. While the effect of pH on hIAPP toxicity has not been directly studied *in vivo*, the use of mutants to simulate the effect of hIAPP protonation has been performed.[77,78,79] The only residue that can be titrated over the pH range hIAPP experiences *in vivo* is H18, with a pK_a near 6.5 in the unstructured monomer. Interestingly, replacing the positively charged R18 in the non-amyloidogenic rat IAPP (rIAPP, Fig. 5) with H18 (that is, R18H) is sufficient to allow fibrillization of rIAPP, albeit to a decreased degree when compared to the human variant.[77]

In addition to fibrillization effects caused by protonation state of the 18th residue, a H18R mutation in the membrane-binding *N*-terminal fragment of hIAPP (the mutant is the same as *N*-terminal fragment of rIAPP) has been shown to decrease membrane insertion and associated cellular toxicity.[78] In the absence of comprehensive studies on the effect of pH on hIAPP fibrillization-induced toxicity, the histidine to arginine mutation provides indirect evidence for the role of charge state of the 18th residue and subsequent effects on aggregation and toxicity. A recent study has shown that the H18R mutants in the non-amyloidogenic, yet toxic, hIAPP$_{1-19}$ fragment results in alternate interaction with model

membranes.[78] $hIAPP_{1-19}$ incubated with DMPC/DMPG in a ratio of 7:3 (DMPC = dimyristoylphosphatidylcholine; DMPG = dimyristoylphosphatidylglycerol) has a smaller effect on the thermodynamic parameters of the gel to liquid-crystalline phase transition than the H18R mutant (or $rIAPP_{1-19}$), as determined by differential scanning calorimetry (DSC), suggesting $hIAPP_{1-19}$ is inserting deeper into the membrane than $rIAPP_{1-19}$.[79] The mechanistic differences described likely correlate with physiological events as the $hIAPP_{1-19}$ fragment was shown to disrupt Ca(II) homeostasis (a relative indicator of cell viability)[79] of islet cells to a greater extent than $rIAPP_{1-19}$.

In addition to the charge-induced differences in insertion and permeability that have been identified, there are aggregation-related cytotoxicity mechanisms that arise when the pH is altered. Current models of hIAPP-induced membrane disruption suggest that either aggregation intermediates (*e.g.*, oligomers) are the most toxic species or the process of fibrillization is the primary cause of membrane disruption.[8,80] Since the $hIAPP_{1-19}$ model fragment is non-amyloidogenic, the study was not able to probe the fibrillization-dependent toxicity and it is not clear if this truncated fragment forms the same oligomers as the full-length peptide. The low pH of the secretory granule likely affects the oligomerization and aggregation mechanisms as electron micrographs have shown that fibrils formed at low pH are morphologically different from those formed at neutral pH.[81,82] The specific difference in the morphologies of hIAPP fibrils at varying pHs, however, are highly dependent on the experimental conditions. For example, Abedini and Raleigh observed aggregates grown at pH 8.8 readily produce protofibrils and those grown at pH 4.0 are mainly amorphous aggregates; however, EM images reported by Clark and coworkers presented the formation of short protofibrils under acidic conditions (pH 3) and large aggregates of protofibrils in a slightly basic gel (pH 7.4 and 9).[81,82] The effects of pH on fibrillization can be understood by the proposed β-serpentine model of amyloid fibrils. In the model, hIAPP monomers adopt a conformation between residues 9–37 composed of three planar β-sheet strands arranged in an S shape, with H18 located in the first turn.[83] Incorporation of a positive charge in the first turn would be highly unfavorable, especially as the monomers stack to form fibrils. The pH-dependent change in fibril morphology is therefore related to a new energy minimized conformation in the presence of additional charge on H18.

2.2 Interaction of IAPP with Metal Ions

The misregulation of metal ions in amyloid related diseases has received attention following the discovery of high occurrence of metal ions in amyloid deposits and in amyloidosis patients.[84] The effect of Zn(II) on hIAPP is of particular interest as β cell granules contain millimolar levels of Zn(II), one of the highest levels in the body, and diabetics often exhibit zinc deficiency.[85,86] Zinc is involved in multiple aspects of glucose homeostasis, including paracrine communication, insulin storage, and glucose-stimulated cascades.[87] Given that hIAPP secretion is part of glucose homeostasis, it is not surprising that Zn(II) has a strong effect on hIAPP aggregation, albeit different from that with Aβ; however, the physical basis of the effect is complex.[88]

Zn(II) has an overall inhibitory effect on hIAPP aggregation as determined by EM and ThT fluorescence assay.[84] Fitting the ThT aggregation curve to a sigmoidal function (Fig. 1) reveals that Zn(II) causes a pH and concentration-dependent effect on lag times and elongation rates, which is summarized in Fig. 6.[84] Since H18 is the only residue that changes protonation state between pH 7.5 and 5.5, the pH dependence can be attributed to the protonation of H18, suggesting the binding is localized near H18. NMR confirms this hypothesis by revealing that the greatest chemical shift perturbation accompanying binding of Zn(II) are localized near H18.[84] The discovery of two Zn-binding sites on hIAPP provides an explanation for the concentration dependence of aggregation kinetics, which change sharply after *ca.* 1 mM Zn(II) is added. Electrospray ionization mass spectrometry

(ESI-MS) of hIAPP with Zn(II) reveals the presence of a low micromolar binding site, which is likely localized near H18, and a low millimolar binding site.[89] Isothermal titration calorimetry (ITC) confirms the low micromolar primary binding site and revealed that 4–6 $hIAPP_{1-19}$ monomers coordinate around a single Zn(II). The effect of this multimeric complex on hIAPP aggregation is not clear; however, the decrease in lag times with the addition of Zn(II) at all concentrations (see Fig 6) is associated with enhanced nucleation that may be caused by this complex. It is important to note that the Zn-bound complex may not be structurally related to the oligomeric nucleus, and the decrease in lag time may simply reflect regions of elevated hIAPP concentrations localized near Zn(II).

Further insight into the increased nucleation of hIAPP in the presence of Zn(II) was gained by studying the structure of Zn(II)-bound hIAPP in helix-promoting organic solvents, 2,2,2-trifluoroethanol (TFE) and hexafluoroisopropanol (HFIP) by NMR spectroscopy.[84] The use of helix promoting solvents allows for the study of hypothesized helical conformations of hIAPP that would otherwise be invisible *via* traditional structural determination methodology. Comparison of these determined NMR structures of hIAPP reveals that Zn(II) breaks the α-helix in the middle of the structure, near H18, and induces a kink between the *N*- and *C*-terminal helices (Fig. 7A). The resulting helix-kink-helix motif is of particular interest as it is a proposed conformational intermediate in the aggregation of hIAPP. Furthermore, a similar conformation was observed in the X-ray crystal structure of a hIAPP dimer attached to the maltose binding protein (Fig. 7B).[90]

The decrease in the elongation rate at physiological pH, especially at low Zn(II) concentrations, is likely due to electrostatic repulsion within the fibril if zinc remained bound to hIAPP.[89] The H18 involved in the high affinity binding site would be located in the interior of the fibril, and similar to the effect of protonating H18, binding of Zn(II) to human IAPP near H18 would result in electrostatic repulsion between neighboring β sheets. This would disfavor the formation of mature fibrils and would push the equilibrium toward monomeric or oligomeric states to minimize electrostatic repulsion.[89] A dye displacement assay confirms this hypothesis; simultaneous monitoring of peptide aggregation and fluorescence of the dye revealed that Zn(II) is released when hIAPP aggregates.[89] Probing the mechanisms underlying the low affinity binding site is more challenging since the high affinity site will be occupied first. The kinetic data of hIAPP incubated with Zn(II) at low pH, when the H18 is protonated and likely unavailable for binding, suggests the second binding site increases the fibril growth rate.[84]

Although the influence of Zn(II) on hIAPP aggregation has been determined *in vitro*, the subsequent effect of Zn(II) on hIAPP cytotoxicity remains to be determined. Caution must be taken when attempting to extrapolate the results of *in vitro* effects of Zn(II) on hIAPP as the peptide is exposed to a range of pH and Zn(II) concentrations that would affect aggregation rates: from the low pH and high Zn(II) concentration of the secretory granule to the physiological pH and low Zn(II) concentration outside the cell. Furthermore, interaction between Zn(II) and other cellular components that interact with Zn(II), such as insulin, would likely alter the amount of free Zn(II) accessible to hIAPP. A final factor to consider is that since either hIAPP oligomers or the process of aggregation are considered most toxic to cells, a decrease in fibril formation does not necessarily correlate with reduced toxicity. This distinction became evident in studies of the effect of Cu on hIAPP aggregation and toxicity.

The presence of Cu in amyloid deposits and its ability to catalyze the formation of toxic ROS has promoted investigations on the effect of Cu(II) on hIAPP aggregation. Studies of hIAPP fibrillization with ThT, AFM, and EM have revealed that Cu(II) inhibits the formation of mature hIAPP fibrils.[91] A recent study, however, has shown the presence of Cu(II) with freshly dissolved hIAPP decreases INS-1 rat insulinoma cell viability to a

greater extent than cells incubated with hIAPP only.[92] Cu-induced oxidative stress was ruled out as the cause of toxicity by repeating the cell studies and aggregation kinetics studies with Ni(II).[92] Ni(II) has comparable binding characteristics to Cu(II) and was shown to decrease hIAPP fibril formation to a similar extent; however, Ni(II) does not contribute to the generation of ROS. Addition of hIAPP to INS-1 cells incubated with Cu(II) and those incubated with Ni(II) resulted in a similar decrease in viability, as compared to cells containing only hIAPP.[92] These findings indicate ROS are not the cause of increased toxicity for hIAPP; instead, Cu(II) possibly stabilizes either a toxic intermediate species of hIAPP or a toxic oligomerization-driven process. In the case of Cu(II), a decrease in amyloid formation does not correspond with a decrease in toxicity, a conclusion that emphasis the importance of combining *in vivo* and *in vitro* techniques to understand the role physiological factors play in the progression of amyloid diseases. This conclusion is especially important in the context of the discussed Aβ metal chelation approaches, as understanding the physiological role of metals in type II diabetes is a prerequisite for application of metal chelation therapy

2.3 Interaction of IAPP with Proteins

Secretory granules of β cells contain a variety of additional peptides that are stored with IAPP, some of which likely regulate IAPP aggregation. Among them, insulin and C-peptide are two proteins found in the secretory granule for which their effects on IAPP aggregation have been studied. The maturation pathway of IAPP, insulin, and C-peptide are similar in that the proteins share transcription promoter elements and are synthesized as precursor peptides that undergo post-translational modification.[73] Cellular production of insulin and C-peptide involve the same precursor, an 86-residue proinsulin peptide that is synthesized in the endoplasmic reticulum (Fig. 5). The precursor peptide is then oxidized and packaged in the Golgi apparatus where it undergoes processing to form the mature insulin and C-peptide proteins that are stored at similar concentrations in the secretory granule.[74] Insulin is a hormone protein that exists as a hexamer in the dense center of the granule and its central role in glucose homeostasis has been extensively documented. The physiological role of C-peptide is less understood; however, it has been used to report on the relative amount of insulin secreted since it is not readily uptaken like insulin following secretion.

The centrality of insulin to glucose homeostasis and diabetes has led to significant interest in the insulin-IAPP interaction, making it the most widely studied protein partner of IAPP. Most studies report that insulin has an overall inhibitory effect on hIAPP aggregation, and *in vitro* studies, using dye-filled liposomes that fluoresce upon leakage, have revealed that insulin has an inhibitory effect on hIAPP-induced membrane disruption.[88,93] ThT fluorescence and CD spectroscopy revealed the A-chain of insulin promote hIAPP fibril formation while the B-chain has an inhibitory effect.[94] The interaction interface between insulin and IAPP was then investigated using decamer hIAPP peptide fragments, corresponding to consecutive overlapping sequences of both peptides, revealing that the inhibitory interaction likely occurs between residues 7–16 of hIAPP and the 8–25 of the insulin B-chain.[94]

NMR chemical shift perturbation of rIAPP incubated with insulin revealed the greatest perturbations occurred in the 1–18 region of rIAPP and between residues 10–20 of the insulin B-chain, confirming previous findings.[95] The greatest chemical shift perturbations on rIAPP occur at R11 and R18 (H18 in hIAPP), and the greatest perturbations of the insulin B-chain occur in the E13–L17 region as well as H10 and G20 (Fig. 7A).[95] These findings suggest the interaction is mediated by a salt bridge most likely between the hIAPP arginine and B-chain glutamate.[95]

The interaction is relatively transient as evident by exchange rates between the free and bound rIAPP exceeding 1000 Hz, as determined by CPMG (CPMG = Carr-Purcell-Meiboom-Gill) measurements and a lack of new NOEs (NOE = nuclear Overhauser effect) upon binding.[95] CPMG is an NMR technique for probing molecular dynamics of processes undergoing a slow exchange (milliseconds to microseconds). NOE is an NMR effect with an r^{-6} distance-dependence whereby magnetization is transferred from one set of nuclear spins to another by cross-relaxation. The distance-dependence of the NOE effect is one of the restraints used for NMR structural determination; however, the effect requires mixing times around hundreds of milliseconds for peptides like IAPP. For conformation or exchange processes occurring faster than the NOE magnetization transfer time, which is the case for rIAPP binding insulin, the effect is averaged and additional NOEs will not be visible.

In addition to the primary interaction interface elucidated by NMR, other interaction interfaces likely to play a role as well. Reports of binding between monomeric hIAPP and the hexameric T_6 insulin structure provides evidence that hIAPP interacts with other regions of insulin as well.[73] The inhibitory B-chain residues in the 9–20 region are located inside the T_6 structure and are likely inaccessible to hIAPP (Figs. 8C and 8D), indicating that the observed $_{73}$ interaction between monomeric hIAPP and the T_6 insulin is likely with other insulin residues.

In addition to interactions between monomeric hIAPP with monomeric insulin and between monomeric hIAPP with insulin crystals, monomeric insulin is also able to interact with fibrillar hIAPP; however, insulin is unable to breakdown the hIAPP aggregates.[96] In addition, there is a variation in the reported effects of insulin on hIAPP fibril morphology. Some studies report minimal effect on individual fibril morphology[82,97] while others report formation of amorphous aggregates[96,98] or thinner fibril strands[98] in the presence of insulin. Differences in sample conditions and preparations are likely to contribute significantly to the variation in the reported fibril morphology. Furthermore, the recent finding of insulin's time-dependent effects on hIAPP aggregation adds an additional variable that may further explain the differences in the observed fibril morphology.[99] The study revealed that insulin inhibits fibrillization of hIAPP for only a limited period, approximately six hours, after which insulin accelerates the fibril formation.[99]

The majority of the studies performed on the peptide interactions with hIAPP have been focused on insulin due to its central role in glucose homeostasis; however, the increased awareness of the role of insulin-related peptides in the pathogenesis of type II diabetes has sparked preliminary interest in how those peptides interact with IAPP. Proinsulin and C-peptide are two proteins that have received particular attention as elevated levels of both peptides are correlated with onset and progression of diabetes.[100] While proinsulin constitutes a minor fraction of the secreted insulin, its release is significantly increased in type II diabetics and in patients with impaired glucose tolerance (a pre-diabetic state with a slightly elevated blood glucose level).[100] It is not yet clear whether the increased level of proinsulin in diabetics is due to a defect in the insulin processing machinery or merely the result of increased secretory demand on β cells that results in depletion of mature insulin and thus, the need to secrete immature granules.[100] Preliminary studies on the interaction between hIAPP and proinsulin have revealed weaker binding affinity of proinsulin to hIAPP and reduced inhibition of hIAPP aggregation in the presence of proinsulin as compared to mature insulin.[88,96] This indicates that either proinsulin has a different structure at the interaction interface with hIAPP or there are differences in the flexibility of the proinsulin sequence. Indeed, a comparison of insulin and the insulin sequence in proinsulin reveals structural rigidification of the insulin domain of proinsulin and only minor structural perturbation of residues that would be located on the B-strand of insulin, the hypothesized interaction interface with hIAPP (Fig. 8C).[101]

C-peptide, the other product from proinsulin processing, is stored with hIAPP at concentrations similar to those of insulin, and therefore identification of effects from this peptide on hIAPP aggregation has drawn interest. Similar to insulin, there are variations in the apparent effects of C-peptide on hIAPP fibrillization with some studies reporting minimal effects on hIAPP aggregation[98,102] while others report C-peptide increases aggregation[88,98] or even a slight decreases in hIAPP fibril formation when incubated with a stoichiometric excess of C-peptide;[98] however, the effects of C-peptide appear significantly smaller than those observed by the other factors in this review. It is not clear by which mechanism C-peptide has an effect on hIAPP or whether the variation in described effects is a result of complex interactions between C-peptide and hIAPP, similar to those observed with insulin, or the result of non-specific interactions. The described peptides account for over 80% of the peptides residing in the secretory granule of β cells; however, the peptide mixture in the granules is complex, containing upwards of 100 different peptides, some of which likely have additional roles in IAPP homeostasis that have yet to be elucidated.[74]

Conclusion

AD and type II diabetes represent two aging related amyloid diseases that have different origins but are characterized by the deposition of amyloid protein aggregates containing misfolded Aβ peptides and IAPP, respectively. These aggregates are termed amyloids based on their common structural traits. As discussed in this review, the mechanisms of their generation and aggregation have been partially elucidated, with recent studies providing evidence that local environmental conditions and interactions with metal ions and other existing proteins can directly influence these processes. While biophysical experiments are increasingly used to elucidate the mechanistic details of amyloid aggregation, atomic-level resolution structural information obtained from cutting-edge NMR techniques would be highly valuable in the design of compounds that can be potentially used to treat these amyloid diseases.

The unique properties of amyloid proteins pose a challenge for traditional drug design; however, the significance of AD and type II diabetes drives development of novel therapeutic strategies that are currently limited by the presently unresolved understanding of the etiology of amyloid diseases. Present efforts to clarify the current understanding of these diseases and the factors impacting them are progressing at an encouraging pace. Innovative ideas to apply small molecule-based approaches to define the roles of metal ions in AD discussed in this review could be used as a stepping-stone into similar approaches for other aspects of protein misfolding conditions. It may be possible, for example, to identify ways to further apply chelators and/or their complexes to alleviate toxicity from metal-IAPP as has been attempted for metal-Aβ.[103,104] Fundamental information gleaned from these types of studies could also be beneficial to accelerate drug discovery for both AD and type II diabetes. To successfully accomplish this in the future, however, a full understanding of the pathophysiological relationship between the formation of misfolded proteins, their interactions with other biological components, and the onset and progression of the diseases is compulsory.

Acknowledgments

Research in the Ramamoorthy laboratory is supported by the National Institutes of Health. Research in the Lim laboratory is supported by start-up funding from the University of Michigan, the Alzheimer's Art Quilt Initiative (AAQI), and Alzheimer's Association (NIRG-10-172326) (to M.H.L.).

References

1. Soto C. FEBS Lett. 2001; 498:204–207. [PubMed: 11412858]

2. Soto C. Nat Rev Neurosci. 2003; 4:49–60. [PubMed: 12511861]
3. Ross CA, Poirier MA. Nat Med. 2004; 10:S10–S17. [PubMed: 15272267]
4. Chiti F, Dobson CM. Annu Rev Biochem. 2006; 75:333–366. [PubMed: 16756495]
5. Fändrich M. Cell Mol Life Sci. 2007; 64:2066–2078. [PubMed: 17530168]
6. Harrison RS, Sharpe PC, Singh Y, Fairlie DP. Rev Physiol, Biochem Pharmacol. 2007; 159:1–77. [PubMed: 17846922]
7. Wilson MR, Yerbury JJ, Poon S. Mol BioSyst. 2008; 4:42–52. [PubMed: 18075673]
8. Butterfield SM, Lashuel HA. Angew Chem Int Ed. 2010; 49:5628–5654.
9. Miller Y, Ma B, Nussinov R. Chem Rev. 2010; 110:4820–4838. [PubMed: 20402519]
10. Reinke AA, Gestwicki JE. Chem Biol Drug Des. 2011; 77:399–411. [PubMed: 21457473]
11. Qiang W, Yau W-M, Tycko R. J Am Chem Soc. 2011; 133:4018–4029. [PubMed: 21355554]
12. Bitan G, Kirkitadze MD, Lomakin A, Vollers SS, Benedek GB, Teplow DB. Proc Natl Acad Sci U S A. 2003; 100:330–335. [PubMed: 12506200]
13. Padrick SB, Miranker AD. Biochemistry. 2002; 41:4694–4703. [PubMed: 11926832]
14. Fezoui Y, Teplow DB. J Biol Chem. 2002; 277:36948–36954. [PubMed: 12149256]
15. Necula M, Kayed R, Milton S, Glabe CG. J Biol Chem. 2007; 282:10311–10324. [PubMed: 17284452]
16. Ehrnhoefer DE, Bieschke J, Boeddrich A, Herbst M, Masino L, Lurz R, Engemann S, Pastore A, Wanker EE. Nat Struct Mol Biol. 2008; 15:558–566. [PubMed: 18511942]
17. Kochanek KD, Xu J, Murphy SL, Miniño AM, Kung H-C. Natl Vital Stat Rep. 2011; 59:1–68. [PubMed: 22808755]
18. Janson J, Laedtke T, Parisi JE, O'Brien P, Petersen RC, Butler PC. Diabetes. 2004; 53:474–481. [PubMed: 14747300]
19. Sims-Robinson C, Kim B, Rosko A, Feldman EL. Nat Rev Neurol. 2010; 6:551–559. [PubMed: 20842183]
20. Alzheimer's Association. Alzheimers Dement. 2011; 7:208–244. [PubMed: 21414557]
21. Jakob-Roetne R, Jacobsen H. Angew Chem Int Ed. 2009; 48:3030–3059.
22. Rauk A. Chem Soc Rev. 2009; 38:2698–2715. [PubMed: 19690748]
23. Scott LE, Orvig C. Chem Rev. 2009; 109:4885–4910. [PubMed: 19637926]
24. Bonda DJ, Lee H-g, Blair JA, Zhu X, Perry G, Smith MA. Metallomics. 2011; 3:267–270. [PubMed: 21298161]
25. Bush AI, Tanzi RE. Neurotherapeutics. 2008; 5:421–432. [PubMed: 18625454]
26. Zatta P, Drago D, Bolognin S, Sensi SL. Trends Pharmacol Sci. 2009; 30:346–355. [PubMed: 19540003]
27. Bolognin S, Drago D, Messori L, Zatta P. Med Res Rev. 2009; 29:547–570. [PubMed: 19177468]
28. Hureau C, Faller P. Biochimie. 2009; 91:1212–1217. [PubMed: 19332103]
29. Barnham KJ, Masters CL, Bush AI. Nat Rev Drug Discov. 2004; 3:205–214. [PubMed: 15031734]
30. Gaggelli E, Kozlowski H, Valensin D, Valensin G. Chem Rev. 2006; 106:1995–2044. [PubMed: 16771441]
31. Hardy JA, Higgins GA. Science. 1992; 256:184–185. [PubMed: 1566067]
32. Lichtenthaler SF, Haass C, Steiner H. J Neurochem. 2011; 117:779–796. [PubMed: 21413990]
33. Ciuculescu E-D, Mekmouche Y, Faller P. Chem –Eur J. 2005; 11:903–909. [PubMed: 15593132]
34. Duce JA, Tsatsanis A, Cater MA, James SA, Robb E, Wikhe K, Leong SL, Perez K, Johanssen T, Greenough MA, Cho H-H, Galatis D, Moir RD, Masters CL, McLean C, Tanzi RE, Cappai R, Barnham KJ, Ciccotosto GD, Rogers JT, Bush AI. Cell. 2010; 142:857–867. [PubMed: 20817278]
35. Haass C, Selkoe DJ. Nat Rev Mol Cell Biol. 2007; 8:101–112. [PubMed: 17245412]
36. Lazo ND, Grant MA, Condron MC, Rigby AC, Teplow DB. Protein Sci. 2005; 14:1581–1596. [PubMed: 15930005]
37. Petkova AT, Ishii Y, Balbach JJ, Antzutkin ON, Leapman RD, Delaglio F, Tycko R. Proc Natl Acad Sci U S A. 2002; 99:16742–16747. [PubMed: 12481027]

38. Chimon S, Shaibat MA, Jones CR, Calero DC, Aizezi B, Ishii Y. Nat Struct Mol Biol. 2007; 14:1157–1164. [PubMed: 18059284]
39. Tamano H, Takeda A. Metallomics. 2011; 3:656–661. [PubMed: 21409223]
40. Tõugu V, Tiiman A, Palumaa P. Metallomics. 2011; 3:250–261. [PubMed: 21359283]
41. Frederickson CJ, Koh J-Y, Bush AI. Nat Rev Neurosci. 2005; 6:449–462. [PubMed: 15891778]
42. Faller P. ChemBioChem. 2009; 10:2837–2845. [PubMed: 19877000]
43. Faller P, Hureau C. Dalton Trans. 2009:1080–1094. [PubMed: 19322475]
44. Drew SC, Barnham KJ. Acc Chem Res. 2011 in press. 10.1021/ar200014u
45. Hou L, Zagorski MG. J Am Chem Soc. 2006; 128:9260–9261. [PubMed: 16848423]
46. Himes RA, Park GY, Siluvai GS, Blackburn NJ, Karlin KD. Angew Chem Int Ed. 2008; 47:9084–9087.
47. Feaga HA, Maduka RC, Foster MN, Szalai VA. Inorg Chem. 2011; 50:1614–1618. [PubMed: 21280585]
48. Drew SC, Noble CJ, Masters CL, Hanson GR, Barnham KJ. J Am Chem Soc. 2009; 131:1195–1207. [PubMed: 19119811]
49. Drew SC, Masters CL, Barnham KJ. J Am Chem Soc. 2009; 131:8760–8761. [PubMed: 19496610]
50. Sarell CJ, Wilkinson SR, Viles JH. J Biol Chem. 2010; 285:41533–41540. [PubMed: 20974842]
51. Noy D, Solomonov I, Sinkevich O, Arad T, Kjaer K, Sagi I. J Am Chem Soc. 2008; 130:1376–1383. [PubMed: 18179213]
52. Hureau C, Sasaki I, Gras E, Faller P. ChemBioChem. 2010; 11:950–953. [PubMed: 20401891]
53. Rodríguez-Rodríguez C, Sánchez de Groot N, Rimola Á, Álvarez-Larena A, Lloveras V, Vidal-Gancedo J, Ventura S, Vendrell J, Sodupe M, González-Duarte P. J Am Chem Soc. 2009; 131:1436–1451. [PubMed: 19133767]
54. Choi J-S, Braymer JJ, Nanga RPR, Ramamoorthy A, Lim MH. Proc Natl Acad Sci U S A. 2010; 107:21990–21995. [PubMed: 21131570]
55. Bandyopadhyay S, Huang X, Lahiri DK, Rogers JT. Expert Opin Ther Targets. 2010; 14:1177–1197. [PubMed: 20942746]
56. Chen T, Wang X, He Y, Zhang C, Wu Z, Liao K, Wang J, Guo Z. Inorg Chem. 2009; 48:5801–5809. [PubMed: 19496588]
57. Braymer JJ, DeToma AS, Choi J-S, Ko KS, Lim MH. Int J Alzheimers Dis. 2011:623051.
58. Perez LR, Franz KJ. Dalton Trans. 2010; 39:2177–2187. [PubMed: 20162187]
59. Deraeve C, Boldron C, Maraval A, Mazarguil H, Gornitzka H, Vendier L, Pitié M, Meunier B. Chem –Eur J. 2008; 14:682–696. [PubMed: 17969218]
60. Dickens MG, Franz KJ. ChemBioChem. 2010; 11:59–62. [PubMed: 19937900]
61. Green DE, Bowen ML, Scott LE, Storr T, Merkel M, Böhmerle K, Thompson KH, Patrick BO, Schugar HJ, Orvig C. Dalton Trans. 2010; 39:1604–1615. [PubMed: 20104324]
62. Scott LE, Telpoukhovskaia M, Rodríguez-Rodríguez C, Merkel M, Bowen ML, Page BDG, Green DE, Storr T, Thomas F, Allen DD, Lockman PR, Patrick BO, Adam MJ, Orvig C. Chem Sci. 2011; 2:642–648.
63. Dedeoglu A, Cormier K, Payton S, Tseitlin KA, Kremsky JN, Lai L, Li X, Moir RD, Tanzi RE, Bush AI, Kowall NW, Rogers JT, Huang X. Exp Gerontol. 2004; 39:1641–1649. [PubMed: 15582280]
64. Wu, W-h; Lei, P.; Liu, Q.; Hu, J.; Gunn, AP.; Chen, M-s; Rui, Y-f; Su, X-y; Xie, Z-p; Zhao, Y-F.; Bush, AI.; Li, Y-m. J Biol Chem. 2008; 283:31657–31664. [PubMed: 18728006]
65. Hindo SS, Mancino AM, Braymer JJ, Liu Y, Vivekanandan S, Ramamoorthy A, Lim MH. J Am Chem Soc. 2009; 131:16663–16665. [PubMed: 19877631]
66. Choi J-S, Braymer JJ, Park SK, Mustafa S, Chae J, Lim MH. Metallomics. 2011; 3:284–291. [PubMed: 21210061]
67. DeToma AS, Choi J-S, Braymer JJ, Lim MH. ChemBioChem. 2011; 12:1198–1201. [PubMed: 21538759]
68. Wild S, Roglic G, Green A, Sicree R, King H. Diabetes Care. 2004; 27:1047–1053. [PubMed: 15111519]

69. Katsilambros, N.; Diakoumopoulou, E.; Ioannidis, I.; Liatis, S.; Makrilakis, K.; Tentolouris, N.; Tsapogas, P. Diabetes in Clinical Practice: Questions and Answers from Case Studies. Wiley, West Sussex; England: 2006.
70. Höppener JWM, Ahrén B, Lips CJM. N Engl J Med. 2000; 343:411–419. [PubMed: 10933741]
71. Höppener JWM, Oosterwijk C, Nieuwenhuis MG, Posthuma G, Thijssen JHH, Vroom TM, Ahrén B, Lips CJM. Diabetologia. 1999; 42:427–434. [PubMed: 10230646]
72. Woods SC, Lutz TA, Geary N, Langhans W. Phil Trans R Soc B. 2006; 361:1219–1235. [PubMed: 16815800]
73. Knight JD, Williamson JA, Miranker AD. Protein Sci. 2008; 17:1850–1856. [PubMed: 18765820]
74. Hutton JC. Diabetologia. 1989; 32:271–281. [PubMed: 2526768]
75. Schmittschmitt JP, Scholtz JM. Protein Sci. 2003; 12:2374–2378. [PubMed: 14500896]
76. Fox A, Snollaerts T, Errecart Casanova C, Calciano A, Nogaj LA, Moffet DA. Biochemistry. 2010; 49:7783–7789. [PubMed: 20698575]
77. Green J, Goldsbury C, Mini T, Sunderji S, Frey P, Kistler J, Cooper G, Aebi U. J Mol Biol. 2003; 326:1147–1156. [PubMed: 12589759]
78. Nanga RPR, Brender JR, Xu J, Veglia G, Ramamoorthy A. Biochemistry. 2008; 47:12689–12697. [PubMed: 18989932]
79. Brender JR, Hartman K, Reid KR, Kennedy RT, Ramamoorthy A. Biochemistry. 2008; 47:12680–12688. [PubMed: 18989933]
80. Engel MFM, Khemtémourian L, Kleijer CC, Meeldijk HJD, Jacobs J, Verkleij AJ, de Kruijff B, Killian JA, Höppener JWM. Proc Natl Acad Sci U S A. 2008; 105:6033–6038. [PubMed: 18408164]
81. Abedini A, Raleigh DP. Biochemistry. 2005; 44:16284–16291. [PubMed: 16331989]
82. Chargé SBP, de Koning EJP, Clark A. Biochemistry. 1995; 34:14588–14593. [PubMed: 7578065]
83. Kajava AV, Aebi U, Steven AC. J Mol Biol. 2005; 348:247–252. [PubMed: 15811365]
84. Brender JR, Hartman K, Nanga RPR, Popovych N, de la Salud Bea R, Vivekanandan S, Marsh ENG, Ramamoorthy A. J Am Chem Soc. 2010; 132:8973–8983. [PubMed: 20536124]
85. Foster MC, Leapman RD, Li MX, Atwater I. Biophys J. 1993; 64:525–532. [PubMed: 8457676]
86. Chausmer AB. J Am Coll Nutr. 1998; 17:109–115. [PubMed: 9550453]
87. Taylor CG. BioMetals. 2005; 18:305–312. [PubMed: 16158221]
88. Westermark P, Li Z-C, Westermark GT, Leckström A, Steiner DF. FEBS Lett. 1996; 379:203–206. [PubMed: 8603689]
89. Salamekh S, Brender JR, Hyung S-J, Nanga RPR, Vivekanandan S, Ruotolo BT, Ramamoorthy A. J Mol Biol. 2011; 410:294–306. [PubMed: 21616080]
90. Wiltzius JJW, Sievers SA, Sawaya MR, Eisenberg D. Protein Sci. 2009; 18:1521–1530. [PubMed: 19475663]
91. Ward B, Walker K, Exley C. J Inorg Biochem. 2008; 102:371–375. [PubMed: 18022240]
92. Yu Y-P, Lei P, Hu J, Wu W-H, Zhao Y-F, Li Y-M. Chem Commun. 2010; 46:6909–6911.
93. Brender JR, Lee EL, Hartman K, Wong PT, Ramamoorthy A, Steel DG, Gafni A. Biophys J. 2011; 100:685–692. [PubMed: 21281583]
94. Gilead S, Wolfenson H, Gazit E. Angew Chem Int Ed. 2006; 45:6476–6480.
95. Wei L, Jiang P, Yau YH, Summer H, Shochat SG, Mu Y, Pervushin K. Biochemistry. 2009; 48:2368–2376. [PubMed: 19146426]
96. Jaikaran ETAS, Nilsson MR, Clark A. Biochem J. 2004; 377:709–716. [PubMed: 14565847]
97. Larson JL, Miranker AD. J Mol Biol. 2004; 335:221–231. [PubMed: 14659752]
98. Janciauskiene S, Eriksson S, Carlemalm E, Ahrén B. Biochem Biophys Res Commun. 1997; 236:580–585. [PubMed: 9245692]
99. Cui W, Ma J-w, Lei P, Wu W-h, Yu Y-p, Xiang Y, Tong A-j, Zhao Y-f, Li Y-m. FEBS J. 2009; 276:3365–3371. [PubMed: 19438709]
100. Breuer TGK, Menge BA, Banasch M, Uhl W, Tannapfel A, Schmidt WE, Nauck MA, Meier JJ. Eur J Endocrinol. 2010; 163:551–558. [PubMed: 20679359]

101. Yang Y, Hua Q-x, Liu J, Shimizu EH, Choquette MH, Mackin RB, Weiss MA. J Biol Chem. 2010; 285:7847–7851. [PubMed: 20106974]

102. Kudva YC, Mueske C, Butler PC, Eberhardt NL. Biochem J. 1998; 331:809–813. [PubMed: 9560308]

103. Hu J, Yu Y-P, Cui W, Fang C-L, Wu W-H, Zhao Y-F, Li Y-M. Chem Commun. 2010; 46:8023–8025.

104. Jeong K, Chung WY, Kye YS, Kim D. Bioorg Med Chem. 2010; 18:2598–2601. [PubMed: 20233659]

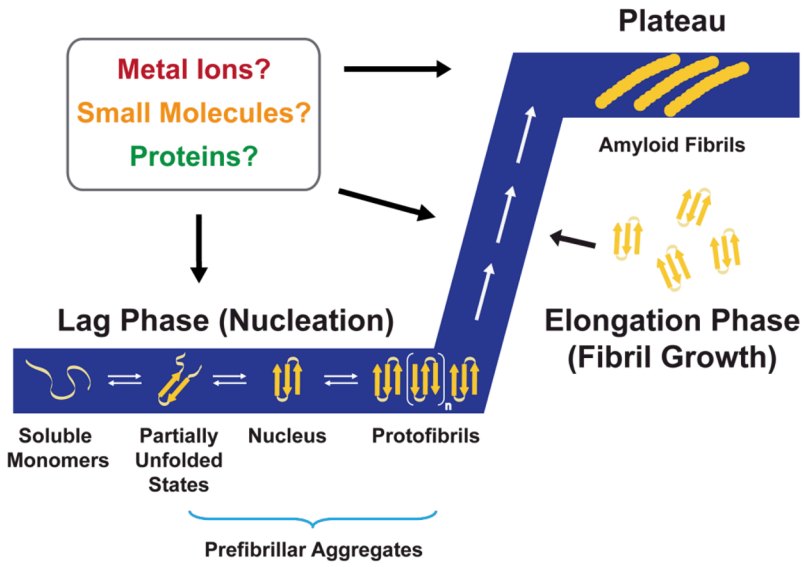

Fig. 1.

Nucleation polymerization model of amyloid aggregation. Soluble monomeric forms of the peptides, such as amyloid-β (Aβ) and islet amyloid polypeptide (IAPP), self-associate during the lag phase (nucleation). This forms a nucleus that can be rapidly extended during the fibril growth period called the elongation phase. Amyloid fibrils are the end product of this process, and their thermodynamic stability allows them to reach a stage called the plateau. The aggregation processes produce a sigmoidal kinetic trace that is depicted in the figure (blue). Additional factors, such as metal ions, small molecules, and other proteins, can be involved at several points during this process and may either facilitate or inhibit this process (see text). This figure is adapted from ref. 7 [reproduced by permission of the Royal Society of Chemistry].

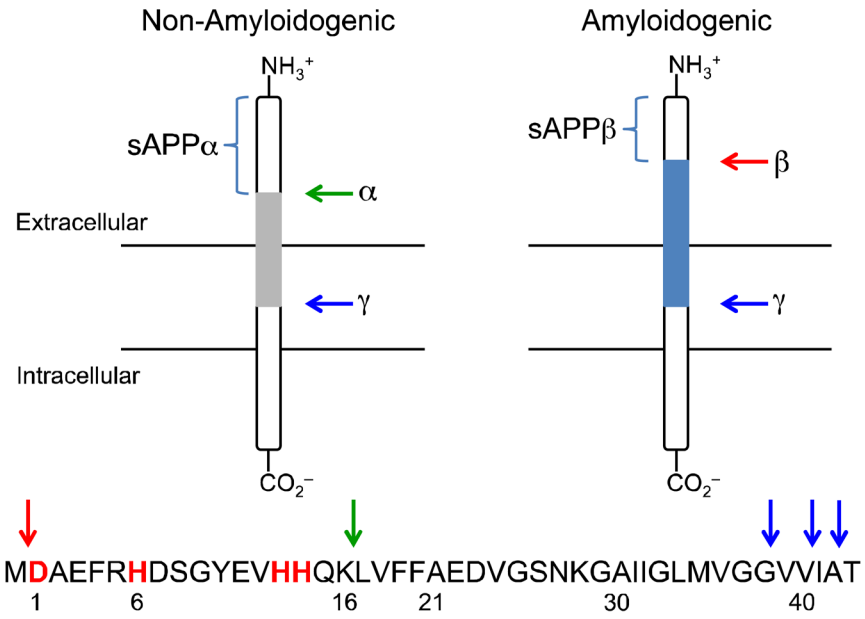

Fig. 2.

Cleavage of APP by α-,β-, and γ-secretases in the non-amyloidogenic and amyloidogenic pathways, respectively. The common full-length peptides, $A\beta_{1-40}$ and $A\beta_{1-42}$, in AD are formed through the amyloidogenic pathway.

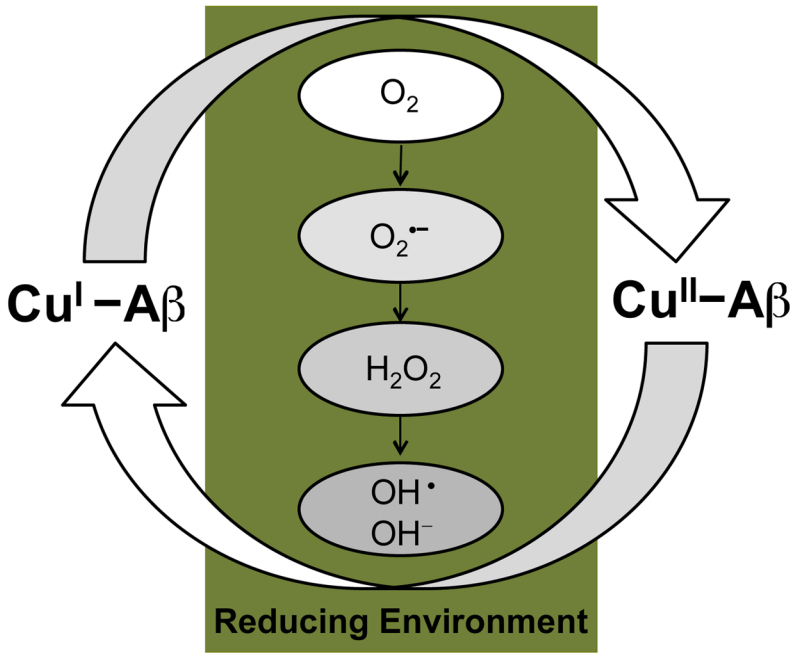

Fig. 3.
ROS generation facilitated by redox cycling of Cu-bound Aβ under reducing conditions (Fenton chemistry).

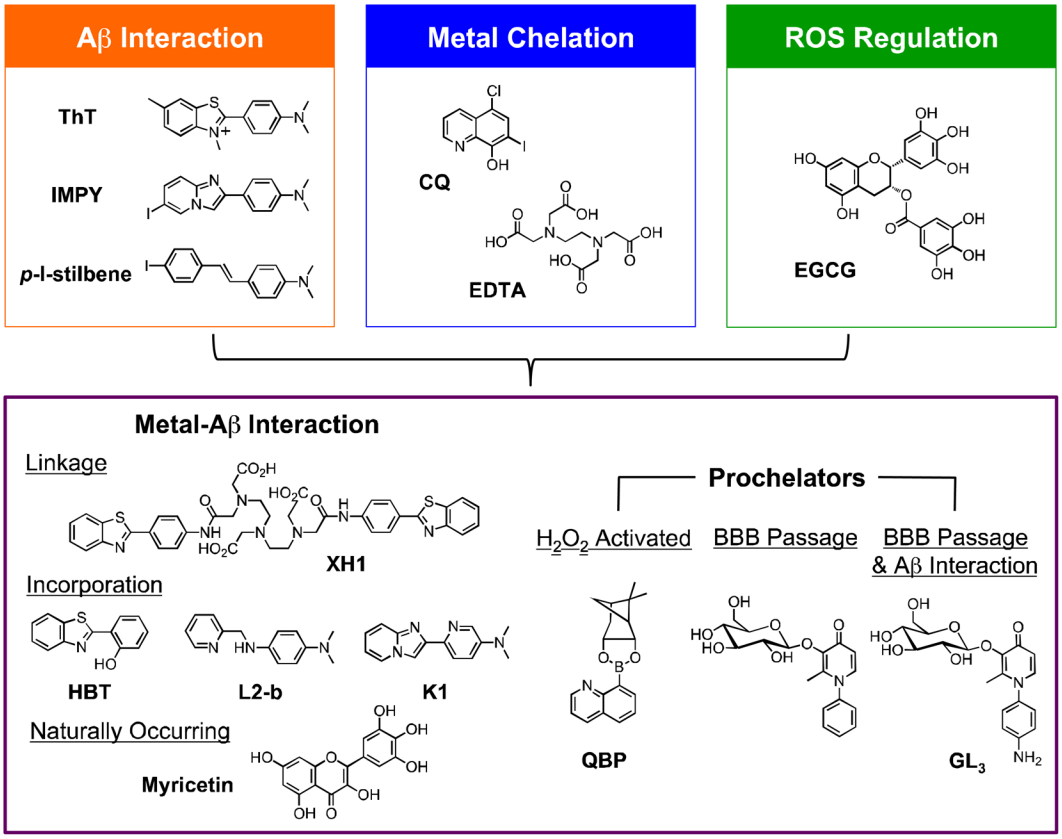

Fig. 4.

Multifunctional small molecules that can be used to investigate Cu(II)/Zn(II)-associated Aβ species in AD by combining properties of Aβ interaction (orange), metal chelation (blue), and/or ROS regulation (green). Other structural moieties can be implemented in the design to introduce different reactivity (*e.g.*, ROS-activated metal chelation ability (prochelators), enhanced BBB permeability). Multifunctional molecules are shown in the purple box. Flavonoids such as EGCG have demonstrated antioxidative properties. Abbreviations for compounds: ThT = thioflavin-T, 2-[4-(dimethylamino)phenyl]-3,6-dimethylbenzothiazolium; IMPY = 6-iodo-2-(4′-dimethylamino)phenylimidazo[1,2-*a*]pyridine; *p*-I-stilbene = *N*,*N*-dimethyl-4-[(1*E*)-2-(4-iodophenyl)ethenyl]benzenamine; CQ = 5-chloro-7-iodo-8-hydroxyquinoline; EDTA = *N*,*N*′-1,2-ethanediylbis[*N*-(carboxymethyl)]glycine; EGCG = epigallocatechin-3-gallate, XH1 = *N*,*N*-bis[2-[[2-[[4-(2-benzothiazolyl)phenyl]amino]-2-oxoethyl](carboxymethyl)amino]ethyl]glycine; HBT = 2-(2-hydroxyphenyl)benzothiazole; L2-b = N^1,N^1-dimethyl-N^4-(pyridin-2-ylmethyl)benzene-1,4-diamine; K1 = 6-(imidazo-[1,2-*a*]pyridin- 2-yl)-*N*,*N*-dimethylpyridin-3-amine; QBP = quinoline boronic acid, pinanediol ester; the prochelator for BBB passage = 3-(D-glucopyranosyloxy)-2-methyl-1-phenyl-4(1*H*)-pyridinone; GL_3 = 1-(4-aminophenyl)-3-(β-D-glucopyranosyloxy)-2-methyl-4(1*H*)-pyridinone.

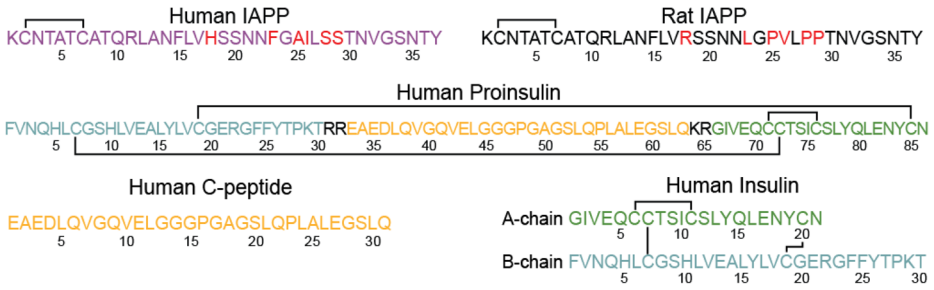

Fig. 5.

Amino acid sequences of IAPP (human and rat), human proinsulin, human C-peptide, and human insulin. Solid lines represent disulfide bonds and residues highlighted in red differ between human and rat IAPP. C-peptide and insulin are cleaved from the same proinsulin fragment, as color-coded, with 4 proinsulin residues removed altogether during processing. Residues highlighted in color in this figure correspond to those in Figs. 7 and 8.

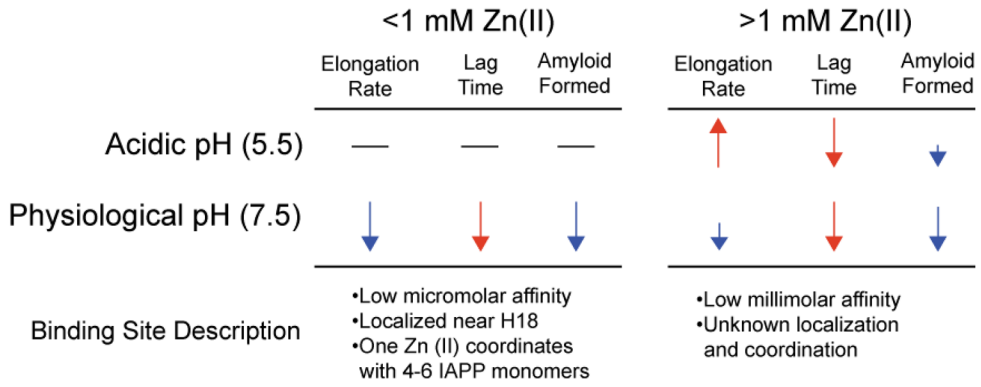

Fig. 6.

Concentration dependent effect of zinc on $hIAPP_{1-37}$ aggregation kinetics and description of the two associated binding sites. Elongation rates, lag time, and relative amyloid formation were obtained by fitting ThT curves to a sigmoidal function. Red arrows correspond to processes that accelerate amyloid formation, blue arrows correspond to processes that inhibit amyloid formation, and dashes signify little change in aggregation kinetics upon addition of Zn(II). Length of arrows corresponds to the magnitude of the effect.

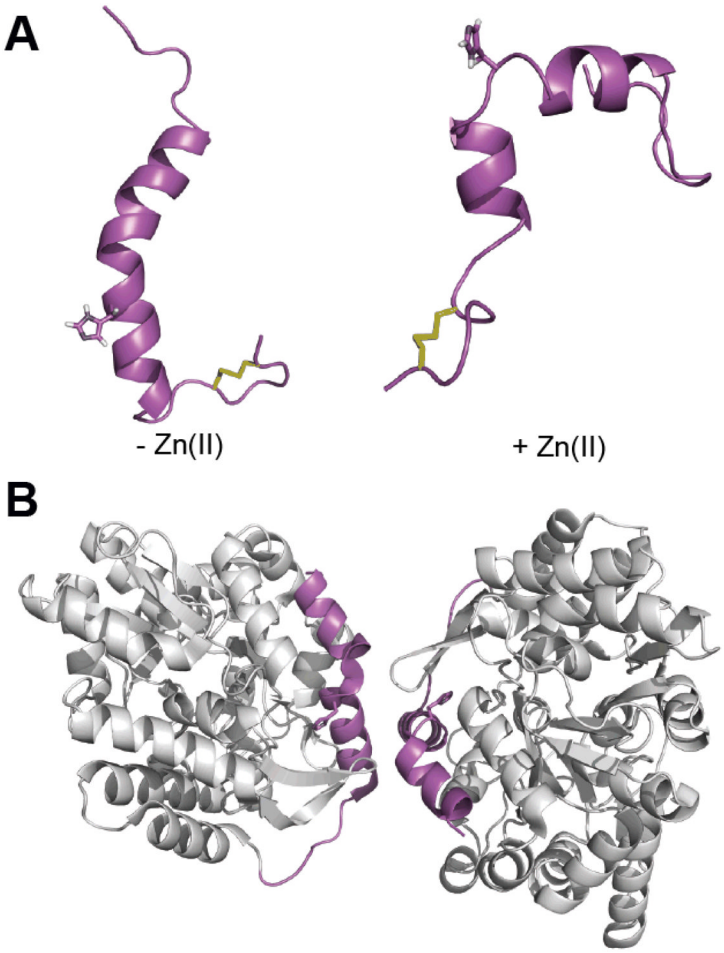

Fig. 7.

Structures of monomeric $hIAPP_{1-37}$ in helix promoting solvent[84] (A) and $hIAPP_{1-29}$–MBP (maltose binding protein) fusion protein dimer (B) (PDB 3G7V). The addition of Zn(II) to monomeric hIAPP in the helical conformation (A) induces a kink near the H18 Zn(II) binding site, resulting in a helix-kink-helix motif that is similar to the helix-kink-helix motif observed in the hIAPP moiety of the fusion protein dimer (magenta in B). The H18 side chain of hIAPP is displayed for reference and disulfide bonds are shown in yellow.

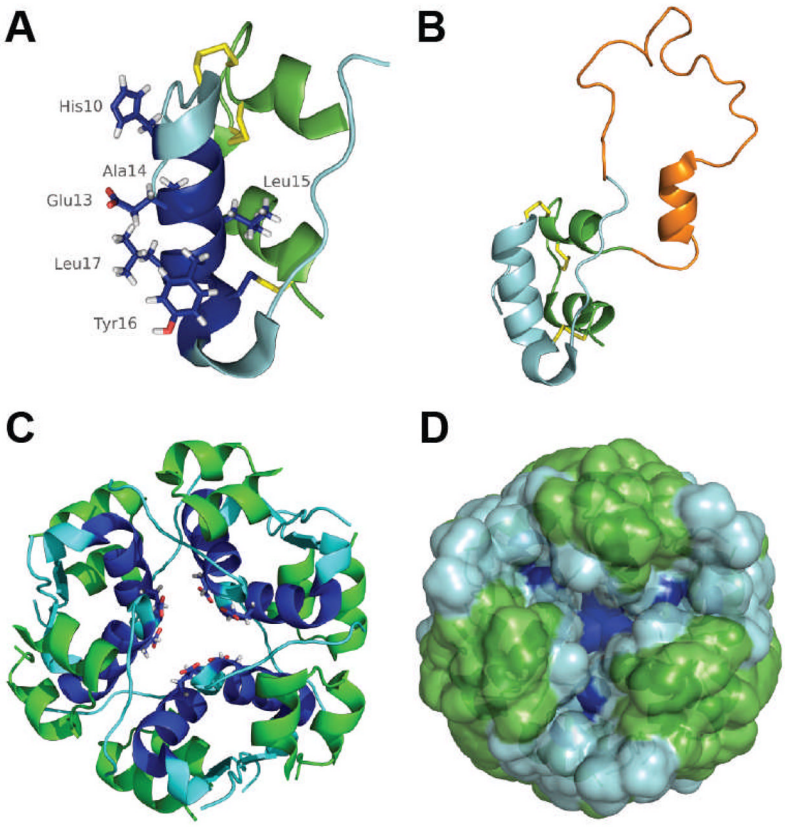

Fig. 8.

Structures of monomeric human insulin (A) (PDB 2JV1), monomeric proinsulin (B) (PDB 2KQP), and human insulin in the hexameric T_6 conformation (C and D) (PDB 1MSO) with similar color schemes. Monomeric insulin is depicted with the A-chain in green, the B-chain in cyan/blue, disulfide bonds in yellow, and the region exhibiting the largest chemical shift perturbations upon binding to rIAPP (residues 10–20) are in blue. Side chains with the greatest chemical shift perturbations are shown as well. The presence of additional residues in proinsulin (orange in B) have little effect on the structure of the insulin moiety in proinsulin (cyan and green). The hypothesized interaction interface between monomeric insulin and IAPP would be located in the interior of the hexameric T_6 insulin storage structure (C and D) and would be inaccessible to IAPP (dark blue with E13 side chain indicated for reference).[73]